Microstructural alterations in the onychomycotic and psoriatic nail: relevance in drug delivery.

Elena Cutrín Gómez[1,2], Soledad Anguiano Igea[1,2], M. Begoña Delgado-Charro[3], José Luis Gómez Amoza[1,2], Francisco J Otero Espinar[1,2]

[1] Department of Pharmacology, Pharmacy and Pharmaceutical Technology. University of Santiago de Compostela

[2] Industrial Pharmacy Institute, University of Santiago de Compostela

[3] Department of Pharmacy and Pharmacology, University of Bath, Bath, BA2 7AY, UK

Corresponding author: M.B. Delgado-Charro

Department of Pharmacy and Pharmacology, University of Bath, Bath, BA2 7AY, UK

E-mail: B.Delgado-Charro@bath.ac.uk

ABSTRACT

Despite the important nail alterations caused by onychomycosis and psoriasis few studies have characterized the microstructure of the diseased nail plate and the diffusion and penetration of drugs through this altered structure. This work aimed to characterize the microstructure of the healthy, onychomycotic and psoriatic human nail using Raman spectroscopy, scanning electron microscopy, optical microscope profilometry and mercury intrusion porosimetry followed by analysis of the structure with PoreCor® software. The results showed that onychomycotic nails have higher porosity and lower amounts of disulfide bonds compared to healthy nails. This suggests that the presence and action of fungi on the nail plate makes this structure more permeable to water and drugs. Psoriatic nails had increased porosity compared to healthy nails but lower than fungal infected specimens. In vitro permeation studies showed that diseased nails were more permeable to ciclopirox (onychomycosis) and clobetasol (psoriasis) although drug permeation was highly variable and likely to be influenced by the degree of alteration of the nail structure. On the whole, this work provides new and valuable information about the microstructure and porosity of diseased nails and a plausible explanation of the increased drug permeability observed in this work and elsewhere.

Keywords: nail, psoriasis, onychomycosis, porosity, ciclopirox, clobetasol propionate

1. INTRODUCTION

Although nail diseases are considered to be minor, they have a relatively high prevalence and a significant impact on the patients' quality of life [1]. Psoriasis is a chronic skin disorder characterized by an abnormal proliferation and differentiation of keratinocytes due to an abnormal immune response. Psoriasis affects about 2-3% of the population and 50% of psoriatic patients have affected nails, which is often related to arthritis in finger joints [2,3]. There are six different

types of lesions in nail psoriasis, the most frequent being pitting of nails (68% of patients) and onycholysis (67%) followed by subungual hyperkeratosis, nail discoloration, nail plate deformations and splinter haemorrhages.

The prevalence of onychomycosis is 2-11% of the general population but the value rises to 20-30% in patients older than 60 years [3–5]. Onychomycosis is caused mainly by dermatophyte infections (90% of cases) primarily *Trichophyton rubrum* followed by *Trichophyton mentagrophyte.* Infections by *Dermatophyte* fungi are due to their ability to colonize keratinized tissues. In particular, fungi penetration is facilitated by production of keratinases that break the keratin of the stratum corneum of the skin and of the nail plate [6]. Nail infections are also caused by yeasts, particularly Candida albicans (8% of infections), and non-dermatophyte molds, e.g., Scopulariopsis brevicaulis (~1-10% of infections) although these fungi show low keratotic activity.

Despite their significant economic, psychological and social impact, nail diseases lack a completely satisfactory treatment. Systemic therapies are usually not recommended for patients with nail psoriasis only but local therapy including topical agents and painful local steroid injections [2,3,7,8] has a high failure rate. In the case of fungal infections, topical treatments have limited success so they are only recommended for mild superficial infections. Systemic antifungal therapies may cause serious side effects and interactions with other drugs [9–11]. One reason behind the failure of topical nail therapies is the composition and structure of the nail plate. This hard structure is primarily made up of hard keratins stabilized by disulfide bridges resulting in a compact structure across which drug molecules diffuse with difficulty [7,12–15]. Brief, this compact structure of the nail plate constitutes the key barrier to drug permeation that hinders the local treatment of nail psoriasis and fungal infection [4,16].

Given the ability of fungi, especially dermatophytes, to modify the structural properties of the nail, it is expected that fungal infection alters the penetration of drugs with respect to healthy nails and potentially, the efficiency of local therapies [16,17]. Yet, little prior work has investigated the penetration of drugs across onychomycotic nails and virtually no data concerning

psoriatic nails are available [16,17]. McAuley et al. [17] measured the penetration of caffeine, amorolfine and terbinafine across onychomycotic nails and tested the use of transonychial water loss measurement (TOWL) as a marker for structural changes of the plate. Surprisingly, despite the presumed increased porosity of infected nails, the TOWL was not significantly different for healthy and infected nails which was potentially explained by the increased thickness of the latter. Only the flux of caffeine, the most hydrophilic drug tested, was correlated to TOWL and nail thickness. According to the authors, the increased porosity of infected nails facilitates diffusion of the more hydrophilic caffeine whereas the transport of the more hydrophobic amorolfine and terbinafine that bind to keratin, is unchanged. However, the porosity of nails was not directly measured in this work. Nair et al. [18] reported that iontophoresis enhanced significantly the penetration of terbinafine across onychomycotic nails compared to passive delivery, however no direct comparison between onychomycotic and healthy nails was made. Baraldi et al. [19] reported that infected nails had increased thickness, reduced density, reduced tensile strength and higher rhodamine permeability than healthy nails. According to the authors, the lower density was due to the increased porosity of diseased nails although, once again, this property was not directly measured.

In previous work [3], we have used SEM and intrusion mercury porosimetry successfully to demonstrate the effect of hydration and chemical enhancers on the microstructure of the nail plate as well as the microstructural differences between human nail and bovine hooves. Further, the microstructure properties determined via mercury intrusion porosimetry and subsequently modeled by Pore-Cor® were related to drug diffusion across nail and hoof.

This work aimed to characterize the structural differences, including porosity, between diseased (onychomycotic and psoriatic) and healthy nails using SEM image analysis, mercury intrusion porosimetry, Raman spectroscopy and profilometry. In addition, the effect of disease on drug ungual penetration was characterized through *in vitro* permeation tests performed with ciclopiroxolamine and clobetasol propionate as model drugs.

2. MATERIALS AND METHODS

2.1. Materials.

Nail samples were sourced from the feet of healthy volunteers and from patients (25-65 years) with onychomycosis and psoriasis. Following informed written consent, healthy volunteers cut their own nails and donated them, infected nails were sourced by several dermatologists from patients with a diagnosis of dermatophytes infection. All samples were washed with distilled water, dried at room temperature and then stored in a glass container at room temperature. Specimens used for ciclopirox olamine diffusion studies were ~8 mm long whereas nail clippings used in all the other studies were approximately 1-3 mm long.

Ciclopirox olamine was supplied by Fagron Iberica (Terrassa, Spain) and clobetasol propionate by Acofarma (Terrassa, Spain). Phosphate buffered saline 0.1M pH 7.4 was prepared accordingly to the European Pharmacopoeia 8th edition from potassium dihydrogen phosphate, sodium dihydrogen phosphate dodecahydrate (VWR, Spain), sodium chloride (Panreac Quimica SA, Spain) and potassium chloride (Panreac Quimica SA, Spain) all of analytical grade. Sodium azide was supplied by Panreac Quimica SA (Barcelona, Spain) and the methanol used to extract ciclopirox and clobetasol from nail samples was provided by Prolabo (Barcelona,Spain).

2.2. SEM analysis.

Healthy and diseased (psoriatic and onychomycotic) nail samples were cut into three pieces of about 1-2 mm long, that were mounted on graphite discs and then coated with copper and gold. After sample preparation, microphotographs were taken using a Zeiss Ultra Plus FESEM microscope and a Zeiss Evo LS 15 SEM Microscope. Images from both the dorsal and ventral surfaces of the nail were taken at randomly selected locations.

The distribution of pore sizes at the nail surface was obtained by image analysis of SEM microphotographs using greyscale images stored in TIFF format. The software package SPIP 4.6.0 (Image Metro-logy A/S, Denmark) was used to determine the distribution of surface pore sizes using Feret diameter as the measurement of the size of superficial pores. An automatic

threshold was used to transform the grayscale image into binary images, that are the images used by the software to calculate the pore size. The results were expressed as “frequency versus pore size” distribution curves that were based on 10-15 images originating from 2-3 nails.

2.3. Mercury intrusion porosimetry (MIP)

Samples of healthy and diseased nails were analysed using a Micromeritics Autopore IV porosimeter (Norcross GA, USA) equipped a penetrometer with 3 ml capacity and a pressure range from 0.004 to 172.4 MPa. Nail specimens were combined to provide the 0.6 g of nail sample used for each MIP study. Depending on the size of the nail clippings the 0.6 g sample could amount to as many as 50-60 specimens. Because collecting these many samples, particularly diseased specimens, was challenging, only one cumulative mercury intrusion curves per nail type was done. The pore size distribution data were then modeled using Pore-Cor™ 6.11 software (Environmental and Fluid Modelling Group, University of Plymouth, UK) [20] which generates an empty three-dimensional structure with characteristics of percolation similar to those of the sample characterized experimentally by MIP [21,22].

A parameter indicating the level of correlation was assigned to the simulated structure above depending on the regularity of arrangement which has values between 0 (random spatial arrangement) and 1 (maximum order of banding) [21].

2.4. Raman Spectroscopy

Raman spectroscopy was performed on healthy, psoriatic and onychomychotic nails (1- 2 mm size) in duplicate (n=2) using a Bruker Raman FT Raman Scope. Measurements of the top (dorsal) of the nail were taken at randomly selected locations [23]. The Raman spectra provided information on the functional groups of the nails, allowing a comparison of the chemical composition of healthy and infected nails [3,24].

2.5 Profilometry studies

These studies used samples (~2-3 mm size) from healthy and onychomycotic nails that were placed on a microscopy slide, held in place with an adhesive strip and flattened as much as

possible without compromising integrity of the sample. A S neox non-contact 3D Surface Profiler from SENSOFAR Surface Metrology (Barcelona, Spain) was used in Confocal mode to acquire the 3D images using the Nikon 20X objective. The study was made in triplicate (i.e., three different healthy and onychomycotic nails) and images were taken from three randomly selected sites from the surface of each nail surface. The roughness of the surface was characterized using typical mean 2D and 3D parameters, Sa, and Ra. Ra is one-dimensional amplitude parameter that is the arithmetic average of the roughness profile (ISO 4287) and Sa the arithmetical mean height in the surface (ISO 25178). The 2D parameter is calculated as the average Ra obtained from tree differences line profiles (0.56 mm long) of each image of the surface of the nail. The data analysis used to estimate Sa and Ra introduced a correction to avoid the influence of the nail curvature on the results so the roughness of the surface in and outside the pores was specifically characterized.

2.6 *In vitro* permeation studies

These eleven days long diffusion studies used samples of healthy and onychomycotic nails (~ 5-8 mm long): healthy nails (n=3 for each drug), onychomycotic (n=3 for ciclopirox) and psoriatic nails (n=3 for clobetasol). Psoriatic and onychomycotic nails exhibited different degrees of involvement.

The thickness was measured at different sites of each nail with a micrometer (Mitutuyo) before the experiments and the arithmetic mean of all measurements used as thickness of each nail. Psoriatic and onychomycotic nails were sterilized for 5 min in UV light [25], hydrated for two hours, dried and fitted between two cylindrical adapters made of polytetrafluoroethylene (Mechanizados del Noroeste, Santiago de Compostela, Spain) providing an effective area of diffusion of 0.196 cm^2. The assembled adapters were fitted between the donor and receptor parts of vertical Franz diffusion cells (Vidrafoc, Barcelona, Spain) with a 7mL receiver volume. The dorsal and ventral parts faced the donor and receptor compartments, respectively. The donor contained 500 µl of saturated ciclopirox olamine water solution (14 mg/ml) [7,20] and the receiver contained pH 7.4 phosphate buffered saline to which sodium azide (30 mg/l) was

added to prevent microbiological and algae growth [10]. The receptor compartment was maintained at constant temperature (37±0.5°C). Every 24 hours, 1 mL samples were taken from the receptor and replaced with equal volume of fresh buffer.

Clobetasol propionate diffusion tests were performed as above but using healthy and psoriatic nails (~ 3-4 mm size) and an effective diffusional area of 0.049 cm^2. A saturated clobetasol propionate water solution (0.0125 mg/ml) was used as a donor. The receptor medium was water with 5% of 2-hydroxyproplyl-β-cyclodextrin (Keptose HPB oral grade, Roquette, France) to ensure sink conditions and with sodium azide (30 mg/l).

The drug concentration in the receptor samples was quantified after filtration through nylon filters and dilution 1:1 with NaOH 1M. The later step aimed to dissolve nail fragments potentially released to the receptor and avoid interferences from nail proteins [3]. Ciclopirox quantification was performed by UV spectroscopy [3] (diode array spectrophotometer Hewlett Packard 8452A) at 308 nm [26] and clobetasol quantification by UPLC-LC/MS.

Clobetasol propionate quantification was performed on a MS/MS tandem Waters Xevo® TQD detector linked to an Acquity UPLC® H-Class system (Waters®, Czech Republic). Data were collected and processed by chromatographic software TargetLynxTM Application Manager. Chromatographic separation was performed at 40ºC using an Acquity (Waters®, Czech Republic) BEH C18 column (2.1 x 50 mm, 1.7 µm particle size) using isocratic conditions (water:methanol 20:80) and a flux of 0.5 ml/min. The autosampler was kept at 10 ºC and the volume of injection was 5 µl. Acquisition of mass spectrometric data was performed in multiple reaction monitoring (MRM) mode via positive electrospray ionization, using the ion transitions of m/z 467.1 > 355.1 (Cone voltage 100 V, collision energy 10 V) a with desolvation gas flow of 1100 l/h, cone gas of 80 l/h and capillary voltage of 0.55 kV. The desolvation temperature and source temperature were 450 ºC and 146 ºC, respectively.

The quantity of drug accumulated in the receiver at different times was determined and then normalised by the corresponding (either 0.196 or 0.049 cm^2) area and plotted against time.

The amount of ciclopirox or clobetasol present in the nail specimens at the end of the diffusion experiments was determined. For this, the cells were dismantled and the dorsal side of the nails was carefully cleaned with distilled water and dried with paper towel. The section of nails that had been exposed to the donor was cut into little fragments which were weighed into vials and 5 ml of 5% methanol in water were added. Then the vials were incubated for 6 days at 25°C with agitation to facilitate extraction of the drug. 1 ml of the extract was collected from each vial, filtered through 0.45 μm nylon filters [20,26] and the drugs quantified as described above.

2.7 Confocal studies

All the observations were performed on a LEICA AOBS-SP5X microscope (Leika microsystem, Germany). Healthy, psoriatic and onychomycotic nails (n=3; ~ 3-4 mm size) were mounted into the Franz cells using the same adapter above. The dorsal layer of the nail faced the donor solution which was 6.5% w/v of sodium fluorescein (Sigma-Aldrich, Spain) in water and the exposure lasted 24 h [27]. Images of exposed layer were taken with an ×10 objective using a black background and x-y planar images were every 5 μm. Transversal images were taken at ×10 objective below the surface to avoid possible artefacts caused by the cut of the exposed nails.

3. RESULTS and DISCUSSION.

3.1 Microstructure of the nail surface:

Fig.1 shows scanning electron microscopy images of the dorsal and ventral surfaces of healthy, psoriatic and onychomycotic nails. Micrographs were taken at different magnifications to appreciate the features of each disease and determine more accurately pore sizes and fractures on the nail surface. The healthy nail showed a dense, compact structure and a surface with tiny pores and fractures. In contrast, the nail with mycosis had an irregular aspect

presenting more pores and defects; these are probably associated to keratin degradation following keratolytic activity by dermatophytes. Further, fungal hyphae (cylindrical cellular structures that form the vegetative structure of fungi in asexual reproductive form) characteristic of dermatophyte fungi were present in the nails, being particularly noticeable at the ventral surface of the nails. In two samples of the psoriatic nails, a concomitant fungi infection by non-dermatophytes was observed (Fig.1-4B). The 2-5 μm of size spherical structures observed in infected psoriatic nails could correspond to the characteristic polysaccharide capsules typical of some encapsulated yeast of the genus Cryptococcus. For example, Cryptococcus uniguttulatus, a specie of this genus, was first isolated from an infected human nail by Wolfram and Zach [28] and has low keratolytic activity.

Next, the SEM micrographs were used to estimate the pore size distribution of the dorsal surface of the nail plate. The image analysis software, SPIP, was used to determine the Feret diameter. Fig. 2 shows the extreme differences found between healthy and diseased nails. The Feret diameter distribution of the surface pore at the dorsal surface of healthy nails was well described by a logarithmic normal distribution with a mean Feret diameter of 10 μm. In contrast, the assortment of numerous pores and cracks present in diseased nails was better characterized by multimodal distributions of the Feret diameter of the surface pores. Thus, the data are not directly comparable; further the distribution was truncated in the case of the diseased nails. The larger number of pores and increased surface pore Feret diameter observed in onychomycotic nails is probably due to the keratolitic activity by the infective fungi that could facilitate detachment of onychocytes. In the case of the psoriatic nail, some lesions involve accumulation of parakeratinocytes cells (abnormal keratinocytes containing nucleus) and longitudinal grooves which could lead to increased surface porosity compared to healthy nails although still lower than that of nails with mycosis.

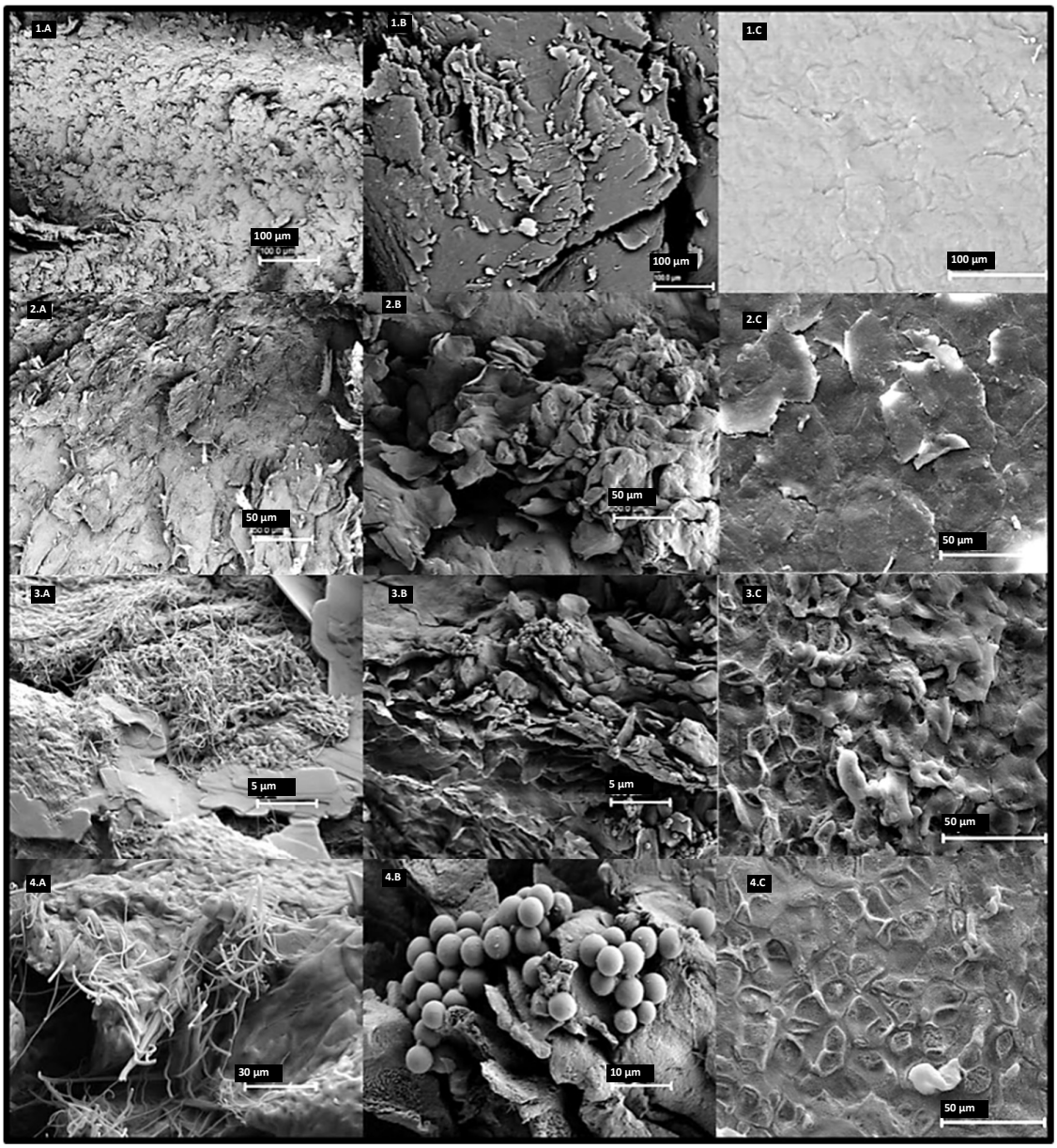

Fig. 1 SEM micrographs of the dorsal (rows 1 and 2) and the ventral (rows 3 and 4) surface of mycotic nails (column A), psoriatic nails (column B) and healthy nails (column C). The bars indicate the magnification used in each case.

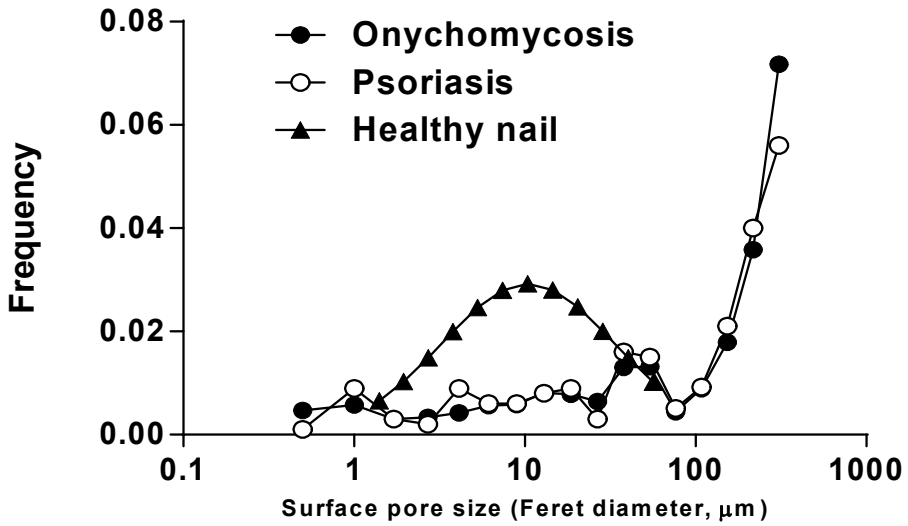

Fig.2 Influence of nail pathology on the size distribution (Feret diameter) of pores at the nail surface.

In addition, non-contact 3D Surface Metrology using continuous confocal techniques were used to characterize further the alterations observed in the surface of infected nails. Figure 3 shows representative images obtained with the optical profilometer. Lines in the images represents the surface profiles used to the determination of the roughness parameters. The colour (left) and grey scale (right) are indicative of different height in the nail surface. The parameters Sa (arithmetical mean height) and Ra (arithmetical mean deviation of the roughness profile) were calculated in accordance with the ISO 25178 and ISO 4287 respectively and used to compare the surface properties of the nails. Determination of the roughness parameters, Ra and Sa, included a correction to avoid the influence of the nail curvature on the determination of the roughness inside and outside the pores. The mean (±SD) Ra and Sa values for three replicates were 1.28 (±0.87) µm and 9.43 (±2.00) µm for healthy nails, respectively and 1.10 (±0.38) µm and 9.96 (±3.35) µm for onychomycotic nails, respectively. No significant changes

were observed in the micro-roughness of the nails with onychomycosis. Nevertheless, the aspect of the nail surface was different for healthy and onychomycotic nails. The 3D surface images of healthy nails remind of their SEM images and the onychocytes are neatly observed on the surface of the plate. This neat organization disappears in the case of mycotic nails, and deformations marks such as cracks and grooves are observed. The combined results in Fig.2 and Fig.3 suggest that diseased nails have more pores but that the surface inside them is relatively smooth.

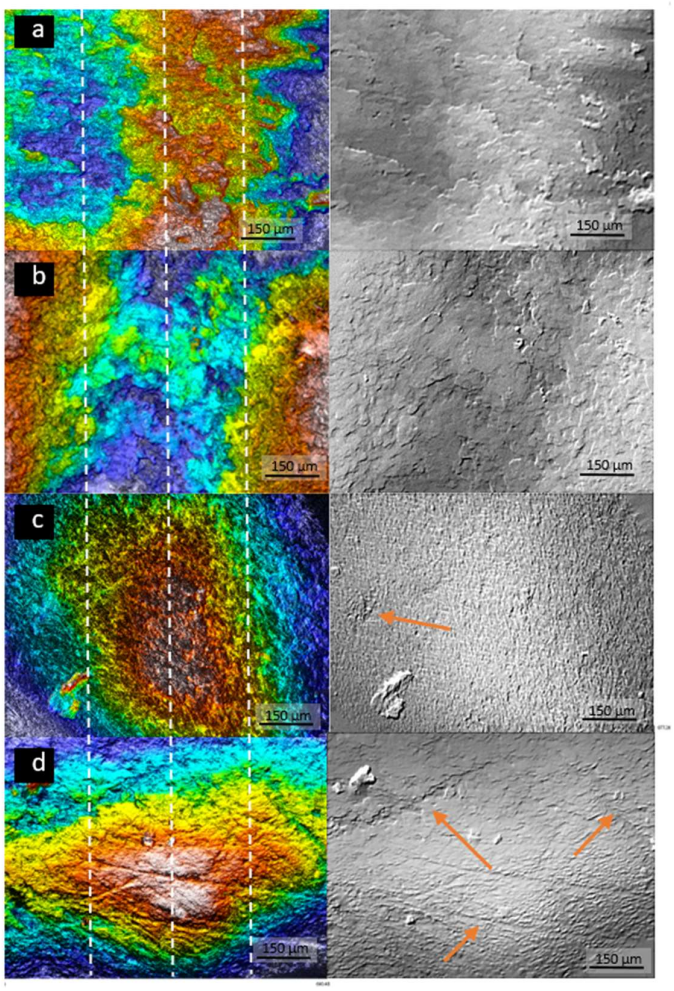

Fig 3. Images of the dorsal surface of the nail obtained by non-contact 3D Surface profilometry using healthy nails (a and b) and onychomycotic nails (c and d). The orange arrows indicate large cracks and grooves in the surface of infected nails.

Hosseinzoi et al. [29] reported that fungal infection modified the roughness of the nail surface. More specifically, the 2D roughness parameter Rq (root mean square roughness determined by AFM techniques) for experimentally infected nails (incubated 14 days with *T. mentagrophytes)* was increased compared with healthy nails, which was due to fungal hyphae populating the nail's surface. Whilst these findings could appear in contradiction to ours the same authors reported that infected nails from patients (as those used in this work) presented a smoother topography than nails infected *ex vivo,* a difference apparently explained by the location where the infection originates. In *ex vivo T. mentagrophytes*-induced onychomycosis, the infection starts from the outer surface of the nail plate whereas *in vivo,* the infection infiltrates the internal side of the nail plate from the nail root and the eponychium [29,30]. This is consistent with our SEM microphotography of naturally infected specimens that showed hyphen in the ventral but not in de dorsal surface of the plate.

3.2 *Microstructure of the internal nail:*

Following characterization of the nail surface, mercury intrusion porosimetry (MIP) was used to characterize the internal microstructure of the nail plate as previously described [19]. The distributions of the pore size presented in Fig. 4 show that healthy and onychomycotic nails presented the lowest and highest porosity, respectively. The distribution of pore diameter obtained for healthy nail microstructure was very similar to the values described by Nogueiras-Nieto in previous work [19].

It could be hypothesized that the higher porosity is related, at least in the case of infected nails, to the keratolytic activity of the fungi. Raman spectra of the dorsal layers of healthy and diseased nails are shown in the supplementary material (Fig.S.1). All samples presented a spectrum typical of a protein-based material. The signals corresponding to disulphide bridges are particularly interesting as they are directly related to the microstructure of the nail. To analyze the data, the ratio of the peak areas corresponding to disulfide bridges with respect to that of C-C bonds was used [24]. The ratios of the peak areas [-SS-/C-C] were 1.13±0.18, 0.86±0.07

and 0.80±0.03 for health, psoriatic and onychomycosis nails, respectively suggesting a significant reduction of disulphide bonds in onychomycotic nails as compared to the healthy nail ($\alpha<0.05$, ANOVA, Sidak's multiple comparisons test) and to a lesser extent (not significant differences) in the case of psoriatic nails. The decrease in the signal intensity of the disulphide bridges is associated with the presence of fungal keratinases that degrade keratin, a process involving breakage of disulphide bridges [31]. In contrast, Baraldi et al., [32] reported that fungal invasion caused little perturbation to disulphide links. This prior work investigated the peaks corresponding to the intact disulfide (S-S group, 430–550 cm^{-1}) and a cleaved disulfide (S-H group, 2550–2600 cm^{-1}) bonds and reported the presence of S-S signals but not –SH peak for onychomycotic nails. The data analysis differed to ours in that the baseline correction and normalization used the Amide I band. Instead, in our case, there was a significant reduction of the ratio [-SS- / C-C] signals for psoriatic and onychomycotic in nails and, in addition, a weak peak at a Raman shift around 2600 cm^{-1} was observed for onychomycotic samples, which was less intense in psoriatic nails. Thus, our data suggest that –SH groups are present in diseased nails but in very low proportion given the weak intensity of the band. To summarize, the significant increase of the nail porosity is due to perturbation in disulphide links and breakage of keratin produced by keratolytic enzymes as well as to the growth and penetration of fungus hyphae in the nail plate and to the onychocyte abnormal proliferation in the case of psoriatic nails.

The pore size distribution determined via MIP was the basis upon which modelling of the porous microstructure of the samples was done using the PoreCor™ 6.31. Pore-Cor™ enables the generation of a three-dimensional void structure that has the same percolation characteristics as the material experimentally characterized by mercury intrusion porosimetry and has been used to characterize nails previously [19].

Fig.5 shows the structure proposed by the modelling software PoreCore for healthy and diseased nails; pores are represented by cubic spaces interconnected by throats (connections) represented by cylinders. In agreement with previous work [19], the model proposed for

healthy nails presents an external region with pores and an internal structure with distinct lower porosity; the latter representing therefore, the strongest barrier to diffusion of chemicals including drugs. The model for onychomycotic nails shows pores of larger size interconnected by wider throats and importantly, this structure is maintained throughout the entire unit cell, i.e., the zone of low porosity is practically absent in infected nails. Finally, the model proposed for psoriatic nails also presented a more porous internal structure than the healthy nail.

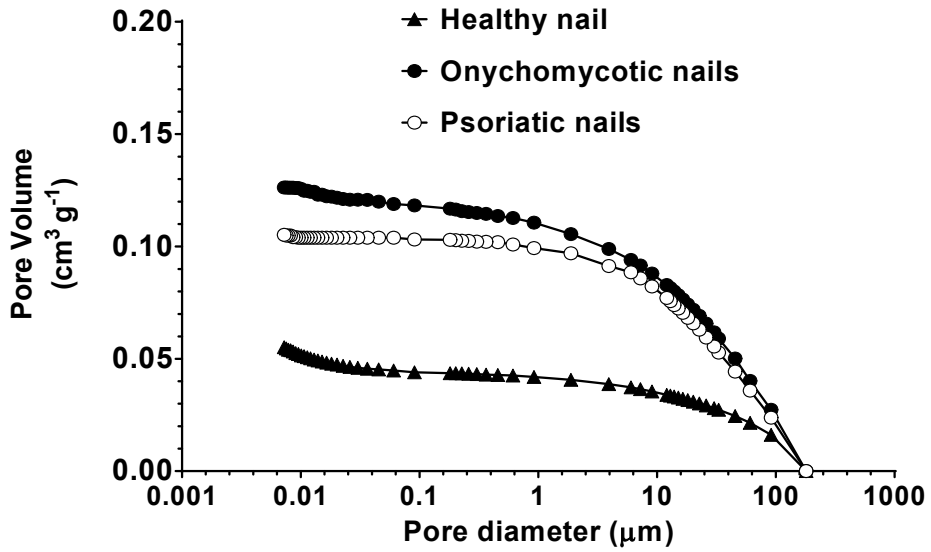

Fig.4 Cumulative curves mercury intrusion for healthy, onychomycosis and psoriatic nails.

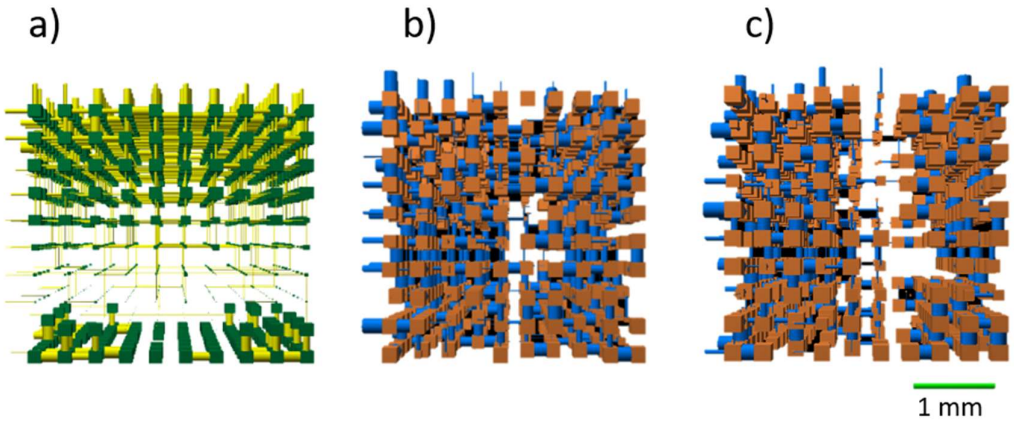

Fig.5. Models proposed by PoreCore™ for the structure of healthy ((a) left panel), mycotic ((b), middle panel) and psoriatic ((c) right panel) nails as based on the pore size distribution determined through mercury intrusion porosimetry. In each cell, the cubes represent pores which are connected by throats represented by the cylinders.

As indicated in the methods section, the correlation level ranges from 0, when the structure is randomized, to 1 when the unit cell is a well-organized structure. The correlation levels found for healthy (0.8), onychomycotic (0.35) and psoriatic (0.12) nails further support the more ordered structure for healthy nails, which presents three zones with different porosity. In contrast, diseased nails have a lower level of correlation, indicating a more random arrangement of pores in their microstructures. The potential implications in drug diffusion are obvious as discussed below. To the best of the authors' knowledge, this is the first report on the pore size distribution at the surface and of the internal porosity of onychomycotic and psoriatic nails. Further, the data presented provides a quantitative evaluation of the degree with which the porosity in diseased nails is increased with respect to that of healthy nails (Fig. 4).

3.3 Implications for drug delivery.

The microstructure of the nail plate, as that of any membrane across which diffusion occurs, is a key determinant of the ease with which actives permeate across this structure and thus, has obvious implications in drug delivery. In the case of the healthy nail, our modelled structure predicts that active ingredients penetrate the outer higher porosity region with less difficulty but then encounter a low porosity internal region which poses a formidable barrier to diffusion. Our experimental observations and the simulated model point out at the intermediate layer of the nail, known for its higher number of disulphide bonds [33], acting as the highest barrier to ungual drug permeation. Interestingly, our data shows that diseased nails present a more porous and homogenous porosity throughout the whole plate which would result in easier penetration of drugs than across the intact structure of the healthy nail.

Fluid permeability is a property of a material indicative of the ease with which a porous material allows the passage of fluids through its structure. PoreCore™ was used to provide an estimate of the permeability of water across the simulated structures. Note that given the differences in geometry between the simulated cells and real nails, these estimates should be taken as a tendency of the percolation characteristics of the systems analysed and not as absolute values for water permeability. The permeability predictions in Fig.6 shows the depth of water penetration into the structure of the nail models obtained with PoreCore™ as a function of time. A first prediction is that water penetrates, at least initially, faster into all the modelled nail structures; this is consistent with experimental data [34] demonstrating the penetration of deuterated water 100 μm into the healthy nail plate in only 35 minutes. A second prediction is the faster penetration into diseased, particularly onychomycotic nails compared to healthy nails. This second prediction is consistent with the higher capacity of water to penetrate into the onychomycotic nail structures reported by McAuley et al. [17].

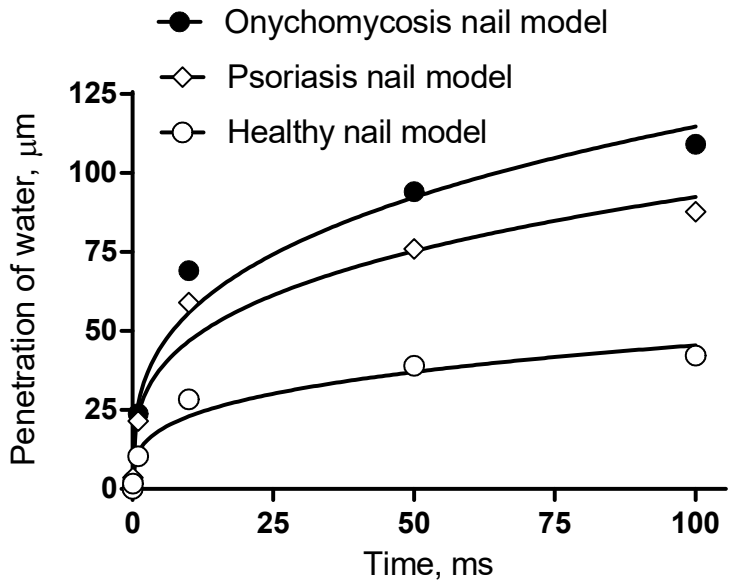

Fig.6. Water penetration kinetics (depth of penetration versus time) into healthy, onychomycosis and psoriasis nail models simulated by the PoreCore™ software.

Finally, a series of *in vitro* permeation studies with fluorescent markers and relevant drugs were done to provide further evidence concerning the different permeation kinetics of xenobiotics across healthy and diseased nails. First, the passive ungual penetration of sodium fluorescein was assessed by laser scanning confocal microscopy to provide qualitative information regarding the depth and uniformity of penetration into the nail plate. The representative images of transversal cuts of the nails following a 24 hours exposure (Fig. 7) show a much greater and deeper penetration of the fluorescent marker into onychomycotic nails; whereas the enhancement was less marked for psoriatic nails. On the whole, these data suggest that the microstructural modifications produced by the pathologies can alter significantly the permeation of drugs.

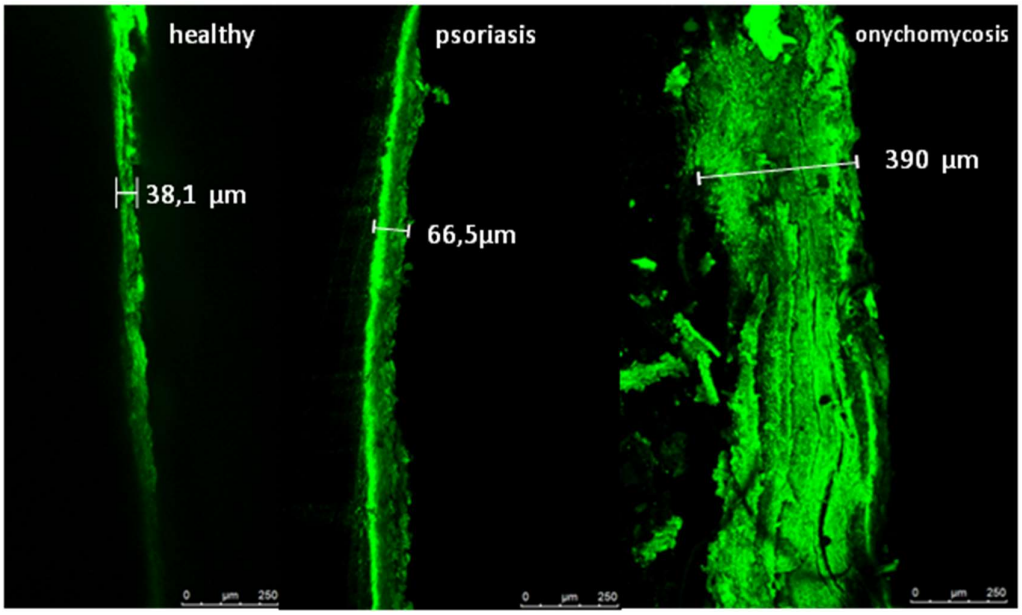

Figure 7. Laser scanning confocal microscopy cross section of healthy psoriatic and onychomycotic nails. Each figure corresponds to one image of a single nail for each pathology. The numbers indicate the penetration depth of the fluorescent marker into the nail plate at the specific location after 24 h of exposure to the fluorescent marker.

Finally, *in vitro* permeation studies (Fig.8) were performed with ciclopirox olamine (antifungal drug used in treatment of onychomycosis) and clobetasol propionate (a corticosteroid prescribed in nail psoriasis) to gather quantitative information with relevant drugs.

The results in Fig.8 show that the two drugs seemed to permeate faster across diseased nails compared to heathy nails. Further, a high inter-nail high variability was observed with permeation being greater for the more severely diseased nails. However, the differences observed did not reach the level of statistical significance. The final percentage of dose permeated was 0.1% and 0.4% of ciclopirox olamine and clobetasol propionate in healthy nails and 0.6% and 7.2% in diseased nails.

The amount (µg) of ciclopirox olamine recovered per mass (g) of nail at the end of the permeation experiments was 3.0±0.6 (2.4-3.5) µg/g and 4.1±1.4 (3.2-5.7) µg/g in healthy and onychomycotic nails, respectively. Larger differences were observed for clobetasol propionate with the recovery being 160±40 (130-210) µg/ g for psoriatic nails and 109±42 (63-142) µg/g nail for healthy nails.

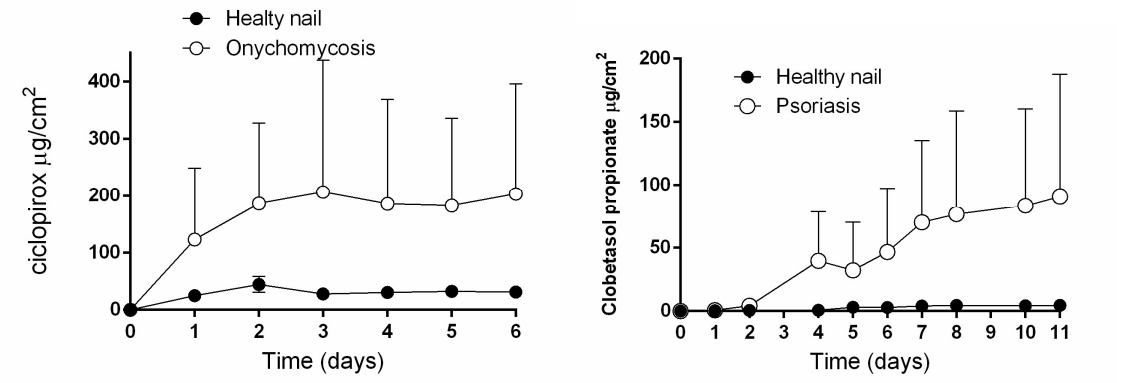

Figure 8. *In vitro* mean (±SD) permeation profiles of ciclopirox (left) and clobetasol propionate (right) across healthy (ciclopirox and clobetasol), onychomycotic (ciclopirox) and psoriatic (clobetasol) nails.

On the whole, the research presented here supports a link between drug diffusion across the nail plate and the microstructure, particularly the porosity, of the membrane. Furthermore, it was shown that onychomycosis and psoriasis modified the microstructure of nails, increasing its porosity and probably leading to increased diffusion. The modifications were particularly remarkable in the case of onychomycosis, where the keratolytic activity of the fungi leads to a porous, random structure with fewer disulfide bridges across which diffusion is much facilitated. It could be argued that the higher penetration of antifungal and psoriatic drugs, particularly in more severe cases could improve the efficiency of these actives and that use of healthy nails in permeation studies underestimates drug penetration. However, as the disease goes into remission and the nail plate regenerates, the structure will become denser and less porous, and less permeable to the passage of drugs. Thus, formulations unable to deliver drug effectively across healthy nails may be effective at initial stages of a treatment but will fail at end stages of the disease. Given the low toxicity expected from topical therapies, it seems judicious to formulate products able to deliver drugs efficiently through the healthy nails as to ensure therapeutic levels complete eradication of the pathology.

CONCLUSIONS

In this work, the surface and overall porosity of diseased nails are reported for the first time. In addition, the significant microstructural alterations produced by onychomycosis and psoriasis on the nail plate were linked to changes in the rate and magnitude of penetration of drugs into and across this membrane. *In vitro* penetration studies with healthy and diseased nails showed a trend for increased permeability of onychomycotic and psoriatic nails towards ciclopirox olamine and clobetasol propionate, respectively. Modelling approaches based on mercury intrusion porosimetry data were successful in predicting these trends suggesting that porosity of the nail plate is a key parameter controlling the ungual diffusion process.

Acknowledgements: Cutrin Gómez thanks the Xunta de Galicia for pre-doctoral funding support.

Declaration of interest

Neither private funding nor involvement with any commercial enterprise were associated with this work.

5. REFERENCES

[1] H.N. Shivakumar, A. Juluri, B.G. Desai, S.N. Murthy, Ungual and transungual drug delivery, Drug Dev. Ind. Pharm. 38 (2012) 901–911. doi:10.3109/03639045.2011.637931.

[2] C. Fischer-Levancini, M. Sánchez-Regaña, F. Llambí, H. Collgros, V. Expósito-Serrano, P. Umbert-Millet, Psoriasis ungueal: tratamiento con ungüento hidrófilo de tazaroteno al 0,1%, Actas Dermo-Sifiliográficas. 103 (2012) 725–728. doi:10.1016/j.ad.2012.04.008.

[3] L. Nogueiras-Nieto, M. Begoña Delgado-Charro, F.J. Otero-Espinar, Thermogelling hydrogels of cyclodextrin/poloxamer polypseudorotaxanes as aqueous-based nail lacquers: application to the delivery of triamcinolone acetonide and ciclopirox olamine, Eur. J. Pharm. Biopharm. 83 (2013) 370–377. doi:10.1016/j.ejpb.2012.11.004.

[4] D. Monti, U. Herranz, L. Dal Bo, A. Subissi, Nail penetration and predicted mycological efficacy of an innovative hydrosoluble ciclopirox nail lacquer vs. a standard amorolfine lacquer in healthy subjects, JEADV. 27 (2013) e153-158. doi:10.1111/j.1468-3083.2012.04529.x.

[5] M.J. Traynor, R.B. Turner, C.R.G. Evans, R.H. Khengar, S.A. Jones, M.B. Brown, Effect of a novel penetration enhancer on the ungual permeation of two antifungal agents, J. Pharm. Pharmacol. 62 (2010) 730–737. doi:10.1211/jpp.62.06.0009.

[6] P. Veer, N.S. Patwardhan, A.S. Damle, Study of onychomycosis: prevailing fungi and pattern of infection, Indian J. Med. Microbiol. 25 (2007) 53–56.

[7] I. Vejnovic, L. Simmler, G. Betz, Investigation of different formulations for drug delivery through the nail plate, Int. J. Pharm. 386 (2010) 185–194. doi:10.1016/j.ijpharm.2009.11.019.

[8] S.N. Murthy, S.R.K. Vaka, S.M. Sammeta, A.B. Nair, TranScreen-N: Method for rapid screening of trans-ungual drug delivery enhancers, J. Pharm. Sci. 98 (2009) 4264–4271. doi:10.1002/jps.21743.

[9] K. Tabara, A.E. Szewczyk, W. Bienias, A. Wojciechowska, M. Pastuszka, M. Oszukowska, A. Kaszuba, Amorolfine vs. ciclopirox – lacquers for the treatment of onychomycosis, Adv. Dermatol. Allergol. Dermatol. Alergol. 32 (2015) 40–45. doi:10.5114/pdia.2014.40968.

[10] I. Kyriakidis, A. Tragiannidis, S. Munchen, A.H. Groll, Clinical hepatotoxicity associated with antifungal agents, Expert Opin. Drug Saf. 16 (2017) 149–165. doi:10.1080/14740338.2017.1270264.

[11] A. Dürrbeck, P. Nenoff, Terbinafine : Relevant drug interactions and their management, Hautarzt Z. Dermatol. Venerol. 67 (2016) 718–723. doi:10.1007/s00105-016-3853-8.

[12] M. Leelavathi, M. Noorlaily, Onychomycosis nailed, J. Acad. Fam. Physicians Malays. 9 (2014) 2–7.

[13] P. Chouhan, T.R. Saini, Hydration of nail plate: a novel screening model for transungual drug permeation enhancers, Int. J. Pharm. 436 (2012) 179–182. doi:10.1016/j.ijpharm.2012.06.020.

[14] D. Monti, L. Saccomani, P. Chetoni, S. Burgalassi, S. Senesi, E. Ghelardi, F. Mailland, Hydrosoluble medicated nail lacquers: in vitro drug permeation and corresponding antimycotic activity, Br. J. Dermatol. 162 (2010) 311–317. doi:10.1111/j.1365-2133.2009.09504.x.

[15] M.M.A. Elsayed, Development of topical therapeutics for management of onychomycosis and other nail disorders: A pharmaceutical perspective, J. Control Release. 199 (2015) 132–144. doi:10.1016/j.jconrel.2014.11.017.

[16] Baraldi, A; Khengar, R. H; Murdan, S; Traynor, M.J; Jones, S. A; Brown, M.B, Chapter 9: The effect of disulphide bond disruption on the barrier integrity of the human nail, in: Adv. Dermatol. Sci., In Chilcott, R and Brain, K ED, 2014: pp. 101–112.

[17] W.J. McAuley, S.A. Jones, M.J. Traynor, S. Guesné, S. Murdan, M.B. Brown, An investigation of how fungal infection influences drug penetration through onychomycosis patient's nail plates, Eur. J. Pharm. Biopharm. 102 (2016) 178–184. doi:10.1016/j.ejpb.2016.03.008.

[18] A.B. Nair, S.R.K. Vaka, S.N. Murthy, Transungual delivery of terbinafine by iontophoresis in onychomycotic nails, Drug Dev. Ind. Pharm. 37 (2011) 1253–1258. doi:10.3109/03639045.2011.568946.

[19] L. Nogueiras-Nieto, J.L. Gómez-Amoza, M.B. Delgado-Charro, F.J. Otero-Espinar, Hydration and N-acetyl-l-cysteine alter the microstructure of human nail and bovine hoof: Implications for drug delivery, J. Control Release. 156 (2011) 337–344. doi:10.1016/j.jconrel.2011.08.021.

[20] G.M. Laudone, G.P. Matthews, P.A.C. Gane, Modelling diffusion from simulated porous structures, Chem. Eng. Sci. 63 (2008) 1987–1996. doi:10.1016/j.ces.2007.12.031.

[21] D.M.W. Peat, G.P. Matthews, P.J. Worsfold, S.C. Jarvis, Simulation of water retention and hydraulic conductivity in soil using a three-dimensional network, Eur. J. Soil Sci. 51 (2000) 65–79. doi:10.1046/j.1365-2389.2000.00294.x.

[22] E. Widjaja, M. Garland, Detection of bio-constituents in complex biological tissue using Raman microscopy. Application to human nail clippings, Talanta. 80 (2010) 1665–1671. doi:10.1016/j.talanta.2009.10.006.

[23] E. Widjaja, G.H. Lim, A. An, A novel method for human gender classification using Raman spectroscopy of fingernail clippings, The Analyst. 133 (2008) 493–498. doi:10.1039/b712389b.

[24] J. Hao, K.A. Smith, S.K. Li, Iontophoretically enhanced ciclopirox delivery into and across human nail plate, J. Pharm. Sci. 98 (2009) 3608–3616. doi:10.1002/jps.21664.

[25] D. Monti, L. Saccomani, P. Chetoni, S. Burgalassi, S. Tampucci, F. Mailland. Validation of bovine hoof slices as a model for infected human toenails: in vitro ciclopirox transungual permeation. Br. J. Dermatol. 165 (2011) 99-105.

[26] J.H. Kim, C.H. Lee, H.K. Choi, A method to measure the amount of drug penetrated across the nail plate, Pharm. Res. 18 (2001) 1468–1471.

[27] J. Dutet, M.B. Delgado-Charro, Assessment of iontophoretic and passive ungual penetration by laser scanning confocal microscopy, Pharm. Res. 29 (2012) 3464–3474. doi:10.1007/s11095-012-0841-2.

[28] K.J. KWON-CHUNG, Perfect State of Cryptococcus uniguttulatus, Int. J. Syst. Evol. Microbiol. 27 (1977) 293–299. doi:10.1099/00207713-27-3-293.

[29] A. Hosseinzoi, F. Galli, L. Incrocci and T. Smijs, Mechanical Properties of Healthy and ex vivo Onychomycosis Nails and the Influence of a Porphyrin-propylene Glycol Antifungal Formulation, Br. J. App. Sci. & Tech. 14 (2016) 1–14. doi:10.9734/BJAST/2016/23177.

[30] S. Goettmann-Bonvallot. Clinical types of onychomycosis, Ann. Dermatol. Venereol. 130 (2003) 1237–1243.

[31] J. Kuner. The digestion of human hair by the dermatophyte microsporum gypseum in a submerged culture. Mykosen. 15 1(972) 59–71.

[32] A. Baraldi, S. A. Jones, S. Guesné, M. J. Traynor, W. J. McAuley, M. B. Brown and S. Murdan. Human nail plate modifications induced by onychomycosis: Implications for topical therapy. Pharm Res. 32 (2015) 1626–1633

[33] D.A. de Berker, J. André, R. Baran. Nail biology and nail science. Int. J. Cosmet. Sci. 29 (2007) 241-275.

[34] W. S. Chiu, N.A. Belsey, N. L. Garrett, J. Moger, M. B. Delgado-Charro, and R. H. Guy. Molecular diffusion in the human nail measured by stimulated Raman scattering microscopy. PNAS. 112 (2015) 7725-7730.